Numerical Methods in Civil Engineering, 7-1 (2022) 28-36

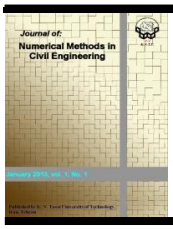

Numerical Methods in Civil Engineering

Journal Homepage: https://nmce.kntu.ac.ir/

# Seismic assessment of a dual concentrically braced steel structure under near-fault ground motions

**Mohsen Tehranizadeh*, Mohsen Khademi** and Amir Shirkhani*****

*ARTICLE INFO*

RESEARCH PAPER

*Article history:*
*Received:*
*February 2022.*
*Revised:*
*March 2022.*
*Accepted:*
*March 2022.*

*Keywords:*
*MRF-CBF dual system,*
*Near-field ground motions,*
*Incremental dynamic analyses,*
*Collapse fragility curve,*
*Global damage index,*
*Pulse period*

***Abstract:***

*In this paper, the seismic performance of a five-story steel structure with a dual system used as a lateral load resisting system comprised of a moment-resisting frame and a concentrically braced frame is evaluated under near-field ground motion records with and without pulses. This research paper aims to evaluate the pulses' effects on the probability of the collapse, global damage index, and the annual and 50-year collapse risks of the structure with such dual systems, which have been less considered in previous research works. To this end, incremental dynamic analyses are performed, and to determine the probability that the studied structure will exceed a specific damage state, fragility functions are developed. The global damage index of the structure is also computed, and a full assessment of the collapse risk of the structure is carried out under the near-field ground motion records with and without pulses. Finally, It is concluded that the probability of collapse, global damage index, and the annual and 50-year collapse risks of the structure subjected to the ground motions with pulses are higher than the ground motions without pulses. For the pulse periods larger than two times the period of the first mode of the structure, the intensification occurs due to the equalization of the increased period of the first mode of the structure and the period of the pulse.*

## 1. Introduction

In recent years, many studies have been carried out to decrease the structural responses by employing different structural systems. These structural systems can be categorized as concentrically braced frames (CBFs), moment-resisting frames (MRFs), and even vibration control systems [1-6]. The main characteristics of the steel CBFs are low-to-medium ductility and high lateral stiffness. The plastic deformation always concentrates in one or a few stories of CBFs, which leads to the weak-story mechanism owing to the decreased plastic redistribution capacity. The main characteristics of the steel MRFs are low lateral stiffness and high ductility.

* *Corresponding Author: Professor, Department of Civil and Environmental Engineering, Amirkabir University of Technology, Tehran, Iran. Email: tehranizadeh@aut.ac.ir*

** *MSc, Department of Civil and Environmental Engineering, Amirkabir University of Technology, Tehran, Iran.*

*** *PhD, Department of Structural Engineering, Faculty of Civil Engineering, University of Tabriz, Tabriz, Iran.*

It has been observed that these traditional systems used in multi-story structures taller than ten stories are vulnerable when they are under long-duration subduction earthquakes [1, 2].

Accordingly, researchers suggested the braced dual structural system that accounts for the MRFs' elastic frame action to diminish CBF systems' weak-story seismic response.

The dual system of ductile flexural walls and ductile space MRF dates back to 1970 (NBCC, 1970). The 1975 edition of NBCC presents a dual system comprising a ductile space MRF and steel bracing or ductile flexural walls designed as follows: The MRF should be designed to resist at least 25% of total base shear and bracing or walls or should be designed to resist 100% of base shear. The same recommendations for the dual structural system are presented in the 1980 and 1985 NBCC editions. In the 1985 edition, it is remarked that the ductile MRF should have the capacity to resist not less than 25% of base shear, but in no case should the ductile MRF have less capacity than that needed according to the relative

rigidities. Since the ductility-related force modification factor (*R*) was presented in the 1990 NBCC edition, each lateral force resisting system is separately defined, but the dual structural system is no longer defined or noted until recently. In Clause 4.1.8.9 (3) of NBCC 2015 [7], it is remarked that for a dual structural system consisting of a moment-resisting frame and a shear wall or braced frame, the lower value of the product $R_d R_0$ is utilized, where $R_0$ and $R_d$ are the overstrength related-force modification factor and the ductility related-force modification factor, respectively. The objective of this clause is to assure that the lateral seismic design force, *V*, is based on the seismic force-resisting system with the lower value of $R_d R_0$, which lead to a higher value of *V*. Therefore, the dual system's response is controlled via its part which has the lower ductility capacity and overstrength. In the same clause of NBCC 2015 [7], it is also noted that the dual structural system must be designed so that 100% of the lateral load is carried by the system with the higher value of $R_d R_0$. If this design procedure is pursued, the other system, which is now not regarded as part of the seismic force-resisting system, shall be designed to maintain its own performance, meaning it should support its gravity loads while experiencing earthquake-induced deformations. In the case that both seismic force-resisting systems of the structural system take part to share the seismic force, both seismic force-resisting systems should be proportioned according to their relative stiffness utilizing structural mechanics principles. For a system comprising seismic force-resisting systems with various *Rd* values, it is important to assure that the less ductile systems can retain displacements related to the more ductile systems without losing their strength. If those structural elements are common to both seismic force-resisting systems, the details of these elements must meet the requirements for the more ductile of the two systems. Kiggins and Uang [8] compared the seismic behavior of a buckling-restrained braced frame (BRB) and a system including a BRB frame and a backup MRF using a three-story and a six-story structure. Using nonlinear dynamic time history analysis (NTHA) with six earthquake records, they deduced that the system reveals a decreased maximum interstory drift and a remarkably lower residual interstory drift. Xie [9] examined the seismic response of the BRB-MRF system with different stiffness ratios allocated to the backup MRF. NTHA was performed on two four-story and twelve-story prototype structures utilizing six earthquake records. It was deduced that by 20% stiffness ratios for the backup MRF, it can diminish the maximum interstory drift. Furthermore, several researchers investigated the seismic response of braced dual systems [10-13] and dual EBF-MRF systems [14, 15]. Design necessities for dual systems are also mentioned in ASCE/SEI 7-10 [16]. The MRFs belonging to the dual system were considered as backup frames to the braced frames and therefore were intended to supply stiffness and strength to prevent the structural collapse in a rare and intense earthquake [17]. To this belief, in the ASCE/SEI 7-10 code, it is determined in Section 12.2.5.1 that "For a dual system, the moment frames should be able to resist at least 25% of the seismic design forces". Incremental dynamic analysis (IDA) is utilized for the comprehensive assessment of the seismic performance of structures [18] within the framework of performance-based earthquake engineering (PBEE). Employing a large number of nonlinear dynamic analyses under a series of multiply scaled earthquake records allows for the detailed evaluation of the seismic behavior of structures for an expansive range of limit states from elasticity to dynamic instability and ultimate collapse. Notwithstanding its enormous computational efforts, IDA has met wide endorsement, and it is being employed ever more by researchers to assess structural performance. For instance, Lee and Foutch [19], Lee and Foutch [20], and Yun et al. [21] used IDA to estimate the collapse capacity of multiple steel MRFs, while Liao et al. [3] and Tagawa et al. [22] conducted IDA to evaluate the performance of several three-dimensional structural models. Pinho et al. [23] used it to assess the precision of pushover analyses on different bridges, and Goulet et al. [24] employed the IDA to evaluate seismic losses for an RC frame structure [25].

Since, up to now, the seismic response of the structures utilizing MRF-CBF dual systems subjected to near-field ground motion records with and without pulses has been less considered, the current research addresses this issue. This paper also aims to evaluate the pulses' effects on the collapse fragility curve, probability of collapse, global damage index, and annual and 50-year collapse risk of a steel structure with an MRF-CBF dual system.

## 2. Incremental dynamic analysis (IDA)

Incremental dynamic analysis (IDA) is a parametric analysis method for the computation of seismic demand and capacity for various levels of intensity measures (IMs) [26, 27]. Performing IDA on structural models requires running dynamic analyses of the model subjected to a series of earthquake records scaled to gradually increasing intensity levels which are suitably selected to force the structure to show its full range of behavior, entirely from elasticity to global dynamic instability [18].

IMs are tools to gauge the ground motion intensity level, e.g., $S_a(T_1,5\%)$ five percent damped first-mode spectral acceleration, while the structural response is commonly described using an engineering demand parameter (EDP), e.g., the maximum interstory drift ratio [28, 29]. Using proper post-processing of the IDA curves, one can specify the distribution of EDP-response for a given IM (or vice-versa), determine proper limit-states, and in combination

with probabilistic seismic hazard analysis [30], specify the mean annual frequency of exceeding selected performance objectives [28]. In this study, the "Hunt and Fill" algorithm is utilized for the IDA procedure [29]. In the Hunt and Fill algorithm, the problem of rapid changes in the number of points allocated to ground motion records commonly used in the fixed step method is solved. Also, due to the curvature of the IDA diagram, the distribution of points is more optimal. In addition, it increases the accuracy of extracting the IM corresponding to the collapse.

## 3. Selected ground motions (GMs)

Nonlinear responses of the structure are evaluated utilizing a set of near-field (NF) ground motions (GMs). This set includes 28 pairs of GMs recorded at sites less than 10 km from fault rupture. The near-field record set comprises two subsets: (i) GMs with strong pulses, called the "NF-Pulse" records, and (ii) GMs without such pulses, called the "NF-No Pulse" records.

## 4. Earthquake hazard levels

In this study, three earthquake hazard levels are considered to evaluate the seismic responses of the structure. These levels are defined based on ASCE/SEI 7-16 [31] for the Site Class D and the San Jose region. The mean return periods (PR) of the hazard levels used in this research are 72, 475, and 2475 yrs. The spectral parameters of the MCE hazard level (PR = 2475 yrs) are $S_s$ = 1.5 and $S_1$ = 0.6 while the site coefficients are $F_a$ = 1.0 and $F_v$ = 1.7. The spectral parameters of the design basis earthquake (DBE) hazard level (PR = 475 yrs) are considered as 2/3 of the parameters' values for the maximum considered earthquake (MCE) hazard level [31-33]. Figure 1 shows the spectra of DBE and MCE earthquake hazard levels in this study. According to ASCE41-06 [34], for the hazard levels with PR < 475 yrs, where $S_s \geq 1.5$, the modified spectral parameters [35] shall be calculated as follows:

$$S_i = S_{i,DBE}\left(\frac{P_R}{475}\right)^n; \quad i = s \text{ or } 1 \tag{1}$$

where $P_R$ is the mean return period at the desired hazard level. Therefore, the parameters' values for the service load earthquake (SLE) hazard level are calculated based on this recommendation.

## 5. Structural design and modeling

A five-story steel structure with an MRF-CBF dual system is considered in this research. The bay width and the story height of this structure are 6.0 m and 3.4 m, respectively. The ASCE/SEI 7-16 [31] standard is used for the general loading. This frame is designed for a high-seismicity area and is based on the requirements of ANSI/AISC 360-10 LRFD [36] and ANSI/AISC 341-16 [37].

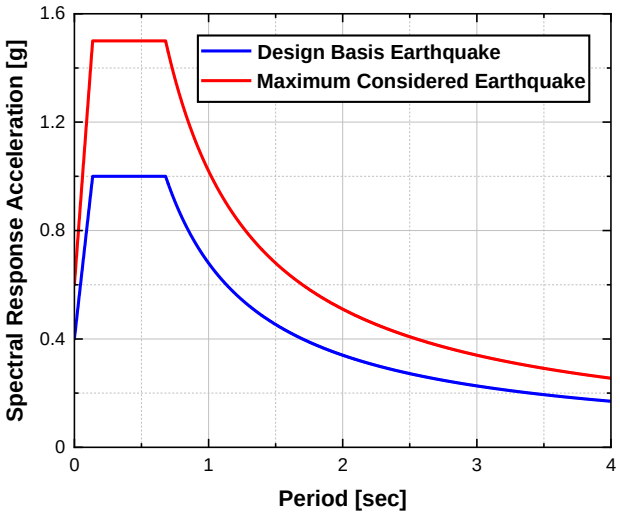


**Fig. 1:** DBE and MCE hazard levels used in this study.

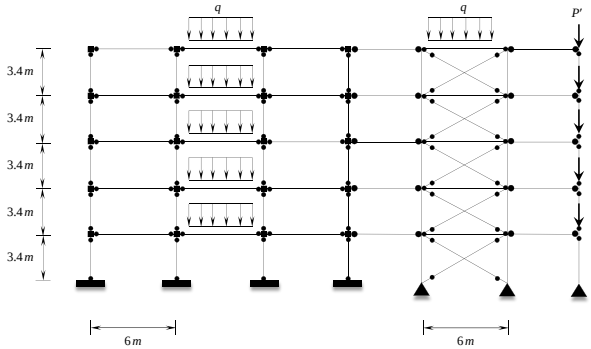


**Fig. 2:** Schematic illustration of the five-story steel structure with an MRF-CBF dual system in this study.

Due to the regularity of the plan of the five-story steel structure considered in this study, two-dimensional models are used to perform nonlinear dynamic analyses. To perform dynamic analyses, the OpenSees software [38] is used. The numerical model of the steel dual system used in this study includes a three-bay special MRF and a single-bay special concentrically braced frame (CBF), as shown in Figure 2. The structural members of MRF are modeled using elastic beam-column elements and, employing plastic hinges, are connected to panel zones. A leaning column is also used to consider the P-Δ effect of the gravity frame. For the special CBF, gusset plate hinges are modeled using the zero-length rotational spring model and Steel02 material. It should also be noted that the recommendations of NIST GCR 17-917-46 (V1 and V3) [39, 40] are used for numerical modeling.

The specifications of the three-dimensional structure from which the two-dimensional frame is selected are given in Table 1.

**Table 1:** Specification of the steel structure with the dual system.

| Number of stories | Total mass (ton) | Design base shear (kN) | Mass participation of 1st mode (%) | Period (sec) |
|---|---|---|---|---|
| 5 | 1636.49 | 2500.10 | 80.70 | 0.629 |

## 6. Analyses and results

To evaluate the seismic responses of the five-story steel structure with the MRF-CBF dual system in this research, NTHA and IDA are used. Figure 3 shows the peak interstory drift ratio (IDR) of the structure for the median NTHA results at different hazard levels used in this research. As shown in the figure, the PIDRs occur in 3rd and 2nd story for SLE, DBE and MCE hazard levels, respectively. The results of the performed IDA for the five-story steel structure with the MRF-CBF dual system are depicted in Figure 4 (a). Here, the IDA results are utilized to acquire fragilities for the five-story steel structure with the MRF-CBF dual system. Fragility functions are employed to quantify the probability that the studied structure will exceed a specific damage state as a function of some IMs. In addition, the probability of collapse on the spectral acceleration level at the first mode period is specified from the IDA results.

The fragility curve is a cumulative distribution function (CDF) of median collapse spectral acceleration from separate GMs. The collapse fragility curve is supposed to follow almost a cumulative lognormal distribution [18, 32, 41, 42]. Figure 4 (b) illustrates the collapse fragility curves of the five-story steel structure with the MRF-CBF dual system. According to the figure, the median and dispersion values for three suites of all NF GMs, NF-Pulse GMs, and NF-No Pulse GMs are (2.513, 0.424), (2.851, 0.449), and (2.216, 0.355), respectively. As it can be seen, due to the pulse effects, for the NF-Pulse GMs, the probability of collapse is more significant than NF-No Pulse GMs for a given spectral acceleration.

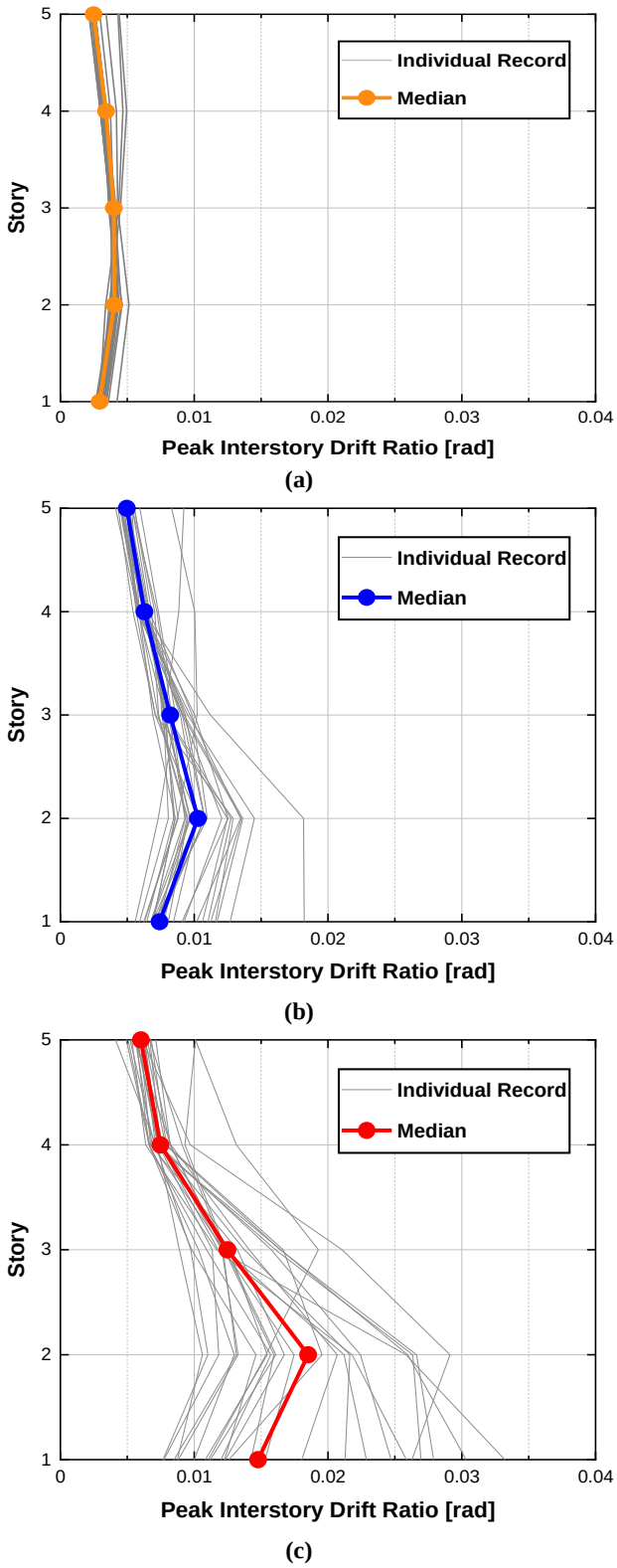


**Fig. 3:** Peak interstory drift ratio (PIDR) of structure at different hazard levels: (a) SLE; (b) DBE; (c) MCE.

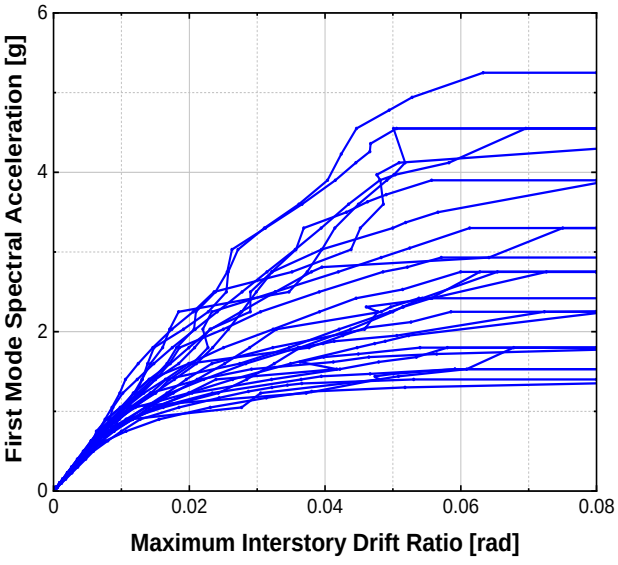


(a)

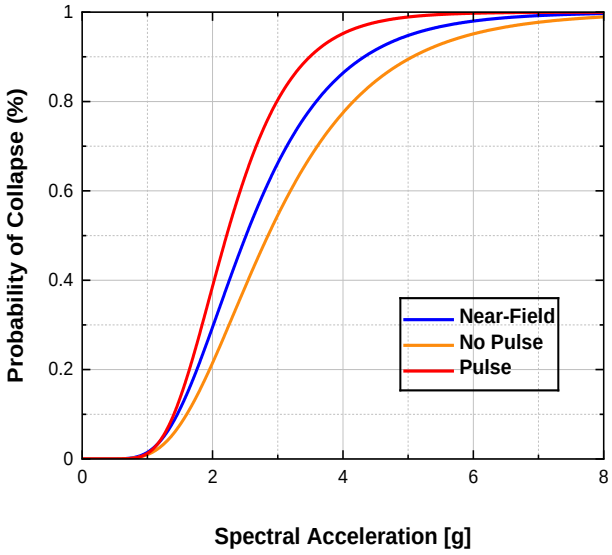


(b)

**Fig. 4:** (a) IDA curves; (b) collapse fragility curves.

As can be seen in Figure 4, the fragility curve of the structure under NF-Pulse GMs is to the left of NF-No Pulse GMs. In other words, NF-Pulse GMs for a given spectral acceleration have more probability of collapsing. For better understanding, the velocity period is calculated for NF-Pulse GMs, as suggested by [43]. Then, for each record, the spectral acceleration of the collapse against the ratio of the structural period to the pulse period is plotted. To make the vertical axis of the diagram in Figure 5 (a) dimensionless, each GM's spectral acceleration of collapse is divided by the median of the spectral acceleration of collapse of NF-No Pulse GMs. In Figure 5 (b), the horizontal axis is the ratio of the pulse period ($T_p$) to the period of the first mode of the structure ($T_1$), and the vertical axis is the ratio of the spectral acceleration of collapse of NF-Pulse GMs the median of the spectral acceleration of collapse of NF-No Pulse GMs.

According to [43], the behavior of the structure at the collapse is affected by the severe nonlinear behavior of the system, and the increase in the structural period is due to the reduction of stiffness. The region $T_p / T_1 > 2$ is the most critical, and it can be stated that the reason for this is intensification due to the equalization of the increased period of the first mode of the structure and the period of the pulse.

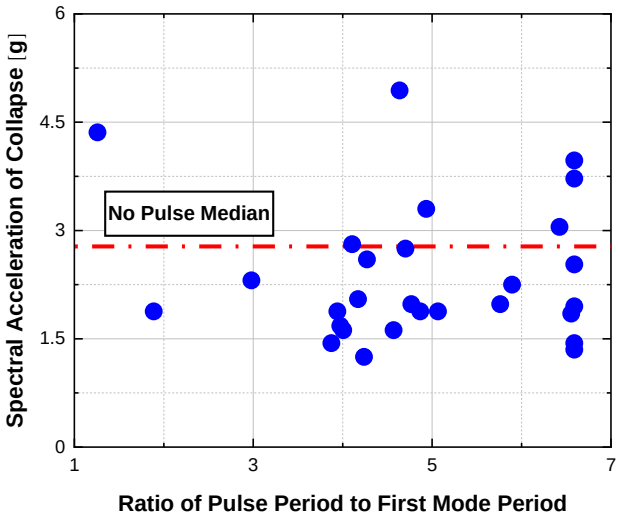


(a)

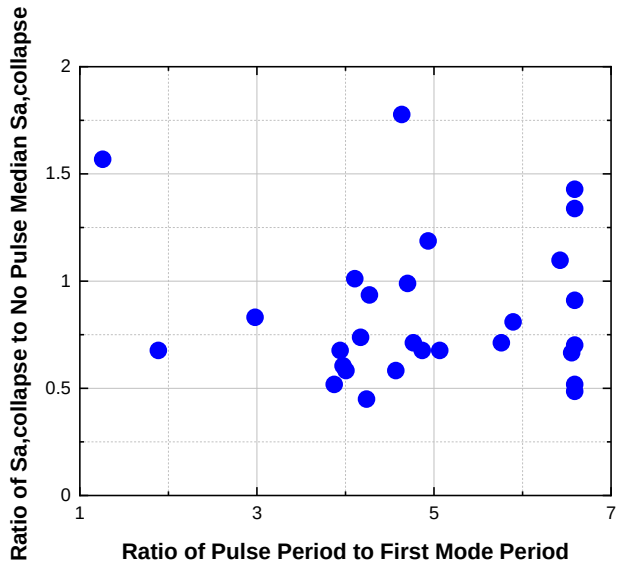


(b)

**Fig. 5:** (a) Spectral acceleration of collapse at the first mode period; (b) ratio of collapse $S_a(T_1)$ to non-pulse median collapse $S_a(T_1)$.

## 7. Local and global damage indices

The seismic performance is evaluated by calculating local and global damage indices. The local damage is determined using the amount of the maximum plastic rotation ($\theta_p^{\max}$)

acquired in the structural members (beam and column elements) of the steel structure. Note that $\theta_p^{\max}$ is a key performance parameter of structural steel components in ASCE/SEI 41-17 [44]. The global damage is determined using a general damage index suggested by Powell and Allahabadi [45]:

$$D_i = \left( \frac{\delta_c - \delta_t}{\delta_u - \delta_t} \right)^m \quad (2)$$

where *m* is an exponent controlling the relationship between the damage parameter and the damage index and $\delta_c$ , $\delta_t$ , and $\delta_u$ are the computed, threshold, and ultimate amounts of the generic damage parameter $\delta$ , respectively. In this research, the interstory inelastic deformation is supposed as the initial damage parameter. The factor *m* is considered equal to 1.5, which is compatible with a low-cycle fatigue procedure, as proposed by Krawinkler and Zohrei [46]. The cumulative damage index at the *i*th story $D_i$ ranges from undamaged (zero) to severely damaged (1.0). In the present research, the threshold damage parameter is depicted using the nominal yield deformation of the *i*th story $\delta_{yi}$ [47-49]. The global damage of the structure is calculated as the weighted average of cumulative damage indices in the following equation at the different story levels, with the weights exhibited by the energy dissipated at the *i*th story $W_{pi}$:

$$D_g = \frac{\sum_{i=1}^{n} D_i . W_{pi}}{\sum_{i=1}^{n} W_{pi}} \quad (3)$$

where *N* is the number of stories. Considering that the energy dissipated corresponding to each story level is proportionate to the damage in that story level, the global damage equation is simplified as follows [47-49]:

$$D_g = \frac{\sum_{j=1}^{n} D_i^2}{\sum_{j=1}^{n} D_i} \quad (4)$$

The nominal yield deformation of the *i*th story $\delta_{yi}$ is computed by a nonlinear static (pushover) analysis of the structure under constant gravity loads and considering an applied monotonically increasing lateral load at the *i*th story only, while lateral supports are imposed on the floor below the *i*th story. This loading pattern minimizes the uncertainties associated with assuming a predefined load pattern such as triangular or uniform as it is particularly focused on the deformation of the *i*th story and interstory force. The lateral load rises in displacement-controlled mode until a peak drift ratio equal to $\delta_{max} / H = 4\%$ (corresponding to the collapse prevention (CP) performance level) and in comparison with the allowable drift of steel MRFs in References [34, 50]. Because of the significant stiffness of the structures with dual systems in comparison with those with moment-resisting frames and due to the lack of information in the available codes about the value of allowable drift of dual systems, in this study, this value is considered equal to 4% based on engineering judgment. To determine the amount of $\delta_{yi}$, an equivalent bilinear elastoplastic relationship with hardening, considering equal energy, is adopted in accordance with the seismic codes [50]. Figure 6 demonstrates the global damage of the five-story steel structure with the MRF-CBF dual system under all NF GMs, NF-Pulse GMs, and NF-No Pulse GMs. As observed in this figure, the percentage of global damage increases with increasing the peak ground acceleration (PGA) level.

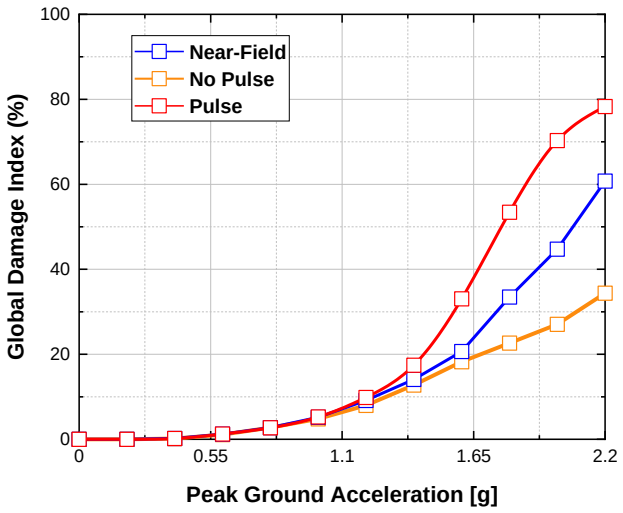


**Fig. 6:** Global damage index of the five-story steel structure with the MRF-CBF dual system obtained by IDA, under all NF GMs, NF-Pulse GMs, and NF-No Pulse GMs.

It can be seen that for the ground motions with pulses, the global damage index of the structure is greater than the ground motions without pulses.

## 8. Collapse risk assessment

To evaluate the annual collapse risk ( $\lambda_F$ ) and the collapse risk in 50 years ( $\lambda_{F(50)}$ ), the mean collapse rate ( $\lambda_c$ ) needs to be computed first. The mean collapse rate can be computed utilizing two components: (i) the seismic hazard curve, which gives the mean annual frequency of exceeding earthquake intensities at the site; and (ii) the fragility curve of the structure, which shows the structure's probability of collapse corresponding to various intensities of the input

earthquake record. Both components shall be integrated utilizing the following equation [51][52]:

$$\lambda_c = \int_0^\infty P(C \mid IM) \cdot \left| d\lambda_{IM}(IM) \right| \quad (5)$$

where $P(C \mid IM)$ is the probability of collapse of the structure when it is excited under an earthquake with the earthquake intensity level of IM, and $\lambda_{IM}$ is the mean annual frequency of exceedance of the earthquake intensity (IM) [51, 52]. Figure 7 shows the seismic hazard curves used in this study. The probability density functions (PDF) derived from collapse fragility curves for all NF GMs, NF-Pulse GMs, and NF-No Pulse GMs are also shown in Figure 8. The annual and 50-year collapse risks of the five-story steel structure with the MRF-CBF dual system are exhibited in Figure 9.

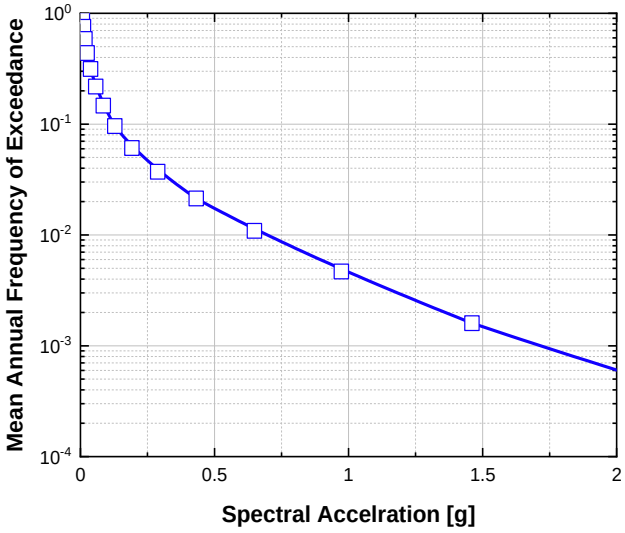


**Fig. 7:** Site-specific hazard curve.

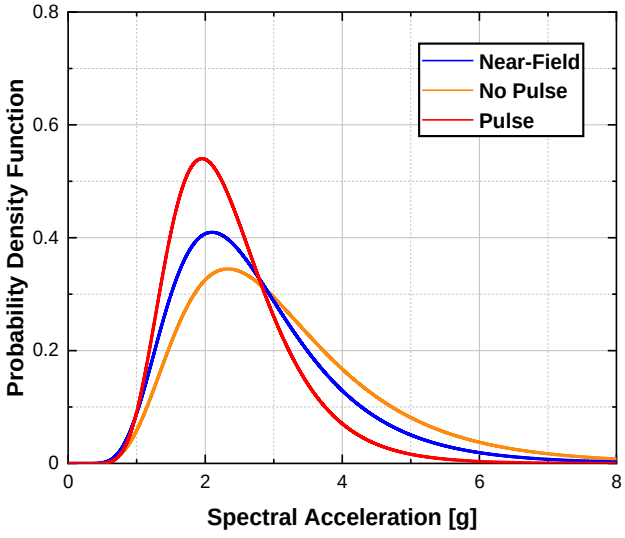


**Fig. 8:** Derivation of collapse fragility curves.

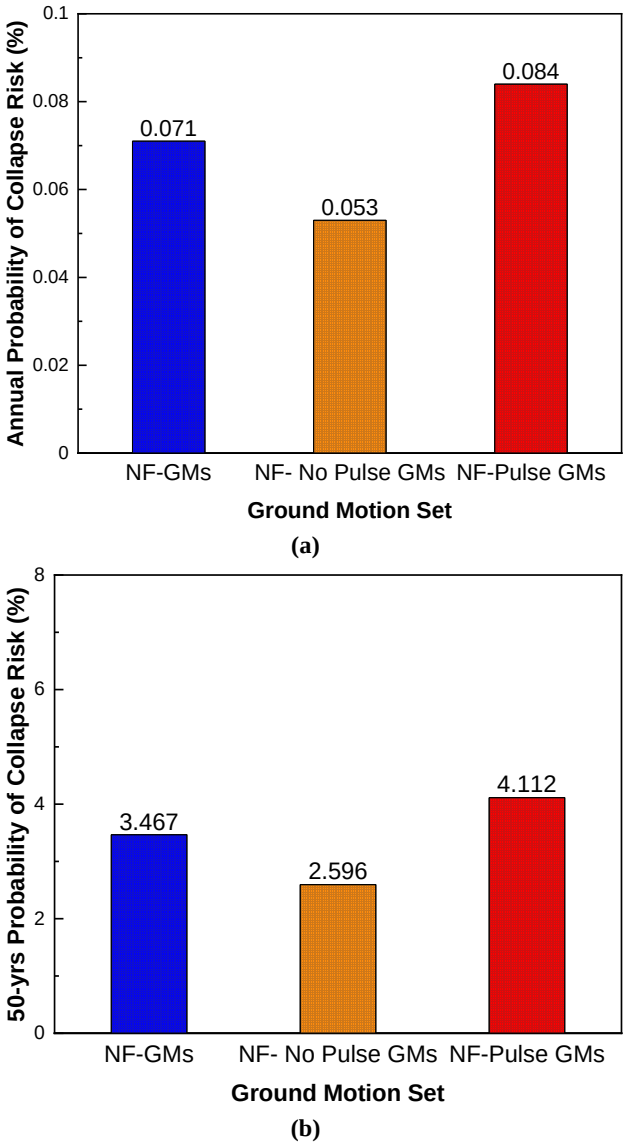


**Fig. 9:** The annual and 50-year collapse risk of the five-story steel structure with MRF-CBF dual system.

As shown in the figure, the annual and 50-year collapse risks of the steel structure with the MRF-CBF dual system under the ground motions with pulses is higher than the ground motions without pulses.

## 7. Conclusions

In this paper, the seismic performance of a five-story steel structure with a dual system comprising a moment-resisting frame and aconcentrically braced frame has been assessed under near-field ground motion records with and without pulses. Such structural systems have been less considered in previous research works.

This paper aims to investigate the effects of the pulseson the probability of the collapse, global damage index, and the annual and 50-year collapse risks of the studied structure.

To this end, incremental dynamic analyses were performed, and to determine the probability that the studied structure

will exceed a specific damage state, fragility functions were developed.

The global damage index of the structure was also computed, and a full assessment of the collapse risk of the structure under the near-field ground motion records with and without pulses was carried out. The findings of this research can be listed as follows:

- Due to the pulse effects, for the ground motions with pulses, the probability of the collapse is greater than the ground motions without pulses for a given spectral acceleration.
- By calculating the global damage of the structure used in this study, it is concluded that the percentage of global damage increases with increasing the peak ground acceleration (PGA) level.
- Owing to the pulse effects, for the ground motions with pulses, the global damage index of the structure is greater than that obtained for the ground motions without pulses.
- For $T_p / T_1 > 2$, the intensification occurs due to the equalization of the increased period of the first mode of the structure and the period of the pulse.
- The annual and 50-year collapse risk of the steel structure with the MRF-CBF dual system subjected to the ground motions with pulses is higher than the ground motions without pulses.

## References

**[1]** Tirca, L., Chen, L., & Tremblay, R. (2015). Assessing Collapse Safety of CBF Buildings Subjected to Crustal and Subduction Earthquakes. Journal of Constructional Steel Research, 115, 47-61.

**[2]** Bosco, M., & Tirca, L. (2017). Numerical Simulation of Steel I-shaped Beams Using a Fiber-based Damage Accumulation Model. Journal of Constructional Steel Research, 133, 241-255.

**[3]** Liao, K. W., Wen, Y. K., & Foutch, D. A. (2007). Evaluation of 3D Steel Moment Frames Under Earthquake Excitations. I: Modeling. Journal of Structural Engineering, 133(3), 462-470.

**[4]** Ebrahimi, A., Edalati, M., Valizadeh, M., & Karimipour, A. (2021). Increase the Effectiveness of AMTMDs and PMTMDs on the Seismic Behaviour of Structures Case Study: Ten-stories Short Period Concrete Building. Engineering Structures, 237, Article e112122.

**[5]** Ghalehnovi, M., Karimipour, A., & Azad Darmian, J. (2019). Study of the Effect of Friction Rotational Damper, Viscoelastic and TADAS on the Structures Seismic Behaviour. Journal of Modeling in Engineering, 17(59), 87-107.

**[6]** Ghalehnovi, & Mansour. (2021). Investigation Responses of the Diagrid Structural System of High-rise Buildings Equipped with Tuned Mass Damper Using New Dynamic Method. Journal of Building Material Science, 1.

**[7]** National Research Council Canada. (2015). National Building Code of Canada 2015.

**[8]** Kiggins, S., & Uang, C. M. (2006). Reducing Residual Drift of Buckling-restrained Braced Frames as a Dual System. Engineering Structures, 28(11), 1525-1532.

**[9]** Xie, Q. (2008). Dual System Design of Steel Frames Incorporating Buckling-Restrained Braces. The 14th World Conference on Earthquake Engineering, Beijing, China.

**[10]** Bosco, M., Marino, E. M., & Rossi, P. P. (2012). Behavior Factor of Dual Concentrically Braced Systems Designed by Eurocode 8. The 15th World Conference on Earthquake Engineering, Lisbon, Porttugal.

**[11]** Giugliano, M. T., Longo, A., Montuori, R., & Piluso, V. (2010). Failure Mode and Drift Control of MRF-CBF Dual Systems. The Open Construction & Building Technology Journal, 4(1).

**[12]** Longo, A., Montuori, R., & Piluso, V. (2014). Theory of Plastic Mechanism Control for MRF–CBF Dual Systems and its Validation. Bulletin of Earthquake Engineering, 12(6), 2745-2775.

**[13]** Longo, A., Montuori, R., & Piluso, V. (2016). Moment Frames–concentrically Braced Frames Dual Systems: Analysis of Different Design Criteria. Structure and Infrastructure Engineering, 12(1), 122-141.

**[14]** Nastri, E., Montuori, R., & Piluso, V. (2015). Seismic Design of MRF-EBF Dual Systems with Vertical Links: EC8 vs Plastic Design. Journal of Earthquake Engineering, 19(3), 480-504.

**[15]** Montuori, R., Nastri, E., & Piluso, V. (2016). Theory of Plastic Mechanism Control for MRF–EBF Dual Systems: Closed Form Solution. Engineering Structures, 118, 287-306.

**[16]** American Society of Civil Engineers(ASCE). (2010). ASCE7-10: Minimum Design Loads for Buildings and Other Structures.

**[17]** American Institute of Steel Construction . (2005).ANSI/AISC360-05: LRFD–Load Resistance Factor Design,–Metric Conversion of the Third Edition.

**[18]** Vamvatsikos, D., & Cornell, C. A. (2002). Incremental Dynamic Analysis. Earthquake Engineering & Structural Dynamics, 31(3), 491-514.

**[19]** Lee, K., & Foutch, D. A. (2002). Seismic Performance Evaluation of Pre-Northridge Steel Frame Buildings with Brittle Connections. Journal of Structural Engineering, 128(4), 546-555.

**[20]** Lee, K., & Foutch, D. A. (2002). Performance Evaluation of New Steel Frame Buildings for Seismic Loads. Earthquake Engineering & Structural Dynamics, 31(3), 653-670.

**[21]** Yun, S. Y., Hamburger, R. O., Cornell, C. A., & Foutch, D. A. (2002). Seismic Performance Evaluation for Steel Moment Frames. Journal of Structural Engineering, 128(4), 534-545.

**[22]** Tagawa, H., MacRae, G., & Lowes, L. (2008). Probabilistic Evaluation of Seismic Performance of 3-story 3D One-and Two-way Steel Moment-frame Structures. Earthquake Engineering & Structural Dynamics, 37(5), 681-696.

**[23]** Pinho, R., Casarotti, C., & Antoniou, S. (2007). A Comparison of Single-run Pushover Analysis Techniques for

Seismic Assessment of Bridges. Earthquake Engineering & Structural Dynamics, 36(10), 1347-1362.

**[24]** Goulet, C. A., Haselton, C. B., Mitrani-Reiser, J., Beck, J. L., Deierlein, G. G., Porter, K. A., & Stewart, J. P. (2007). Evaluation of the Seismic Performance of a Code-conforming Reinforced-concrete Frame Building—from Seismic Hazard to Collapse Safety and Economic Losses. Earthquake Engineering & Structural Dynamics, 36(13), 1973-1997.

**[25]** Wang, Y. (2018). Seismic Performance of Steel Buildings with Braced Dual Configuration and Traditional Frame Systems Through Nonlinear Collapse Simulations. Doctoral dissertation. Concordia University.

**[26]** Mashayekhi, M., Harati, M., Darzi, A., & Estekanchi, H. E. (2020). Incorporation of Strong Motion Duration in Incremental-based Seismic Assessments. Engineering Structures, 223, Article e111144.

**[27]** Harati, M., Mashayekhi, M., Barmchi, M. A., & Estekanchi, H. E. (2019). Influence of Ground Motion Duration on the Structural Response at Multiple Seismic Intensity Levels. Journal of Numerical Methods in Civil Engineering, 3, 10-23.

**[28]** Vamvatsikos, D., & Cornell, C. A. (2004). Applied Incremental Dynamic Analysis. Earthquake Spectra, 20(2), 523-553.

**[29]** Vamvatsikos, D. (2011). Performing Incremental Dynamic Analysis in Parallel. Computers and Structures, 89, 170-80.

**[30]** Cornell, C. A. (1968). Engineering Seismic Risk Analysis. Bulletin of the Seismological Society of America, 58(5), 1583-1606.

**[31]** American Society of Civil Engineers(ASCE). (2016). ASCE7-16: Minimum Design Loads and Associated Criteria for Buildings and Other Structures.

**[32]** Shirkhani, A., Azar, B. F., & Basim, M. C. (2021). Seismic Loss Assessment of Steel Structures Equipped with Rotational Friction Dampers Subjected to Intensifying Dynamic Excitations. Engineering Structures, 238, Article e112233.

**[33]** Shirkhani, A., Azar, B. F., Basim, M. C., & Mashayekhi, M. (2021). Performance-based Optimal Distribution of Viscous Dampers in Structure Using Hysteretic Energy Compatible Endurance Time Excitations. Journal of Numerical Methods in Civil Engineering.

**[34]** American Society of Civil Engineers(ASCE). (2007). ASCE/SEI 41-06: Seismic rehabilitation of Existing Buildings.

**[35]** Foyouzat, M. A., & Estekanchi, H. E. (2016). Application of Rigid-perfectly Plastic Spectra in Improved Seismic Response Assessment by Endurance Time Method. Engineering Structures, 111, 24-35.

**[36]** American Institute of Steel Construction. (2010). ANSI/AISC360-10: Specification for Structural Steel Buildings.

**[37]** American Institute of Steel Construction. (2016). ANSI/AISC341-16: Seismic Provisions for Structural Steel Buildings.

**[38]** Mazzoni, S., McKenna, F., Scott, M. H., Fenves, G. L., & Jeremic, B. (2006). Open System for Earthquake Engineering Simulation (OpenSees). California: Berkeley.

**[39]** Applied Technology Council (ATC). (2017). Guidelines for Nonlinear Structural Analysis for Design of Buildings. Part I – General, NIST GCR 17-917-46v1.

**[40]** Applied Technology Council (ATC). (2017). Guidelines for Nonlinear Structural Analysis for Design of Buildings. Part IIb–Reinforced Concrete Moment Frames, NIST GCR 17-917-46v3.

**[41]** Bradley, B. A., & Dhakal, R. P. (2008). Error Estimation of Closed-form Solution for Annual Rate of Structural Collapse. Earthquake Engineering & Structural Dynamics, 37(15), 1721-1737.

**[42]** Hosseini SA, Banazadeh M. (2021, May 26-29). Collapse Risk Assessment of Mid-Rise to High-Rise Buildings with SMRF Equipped with Viscous Damper (VD) and Buckling-Restrained Brace Frame (BRBF). CSCE 2021 Annual Conference, Las Vegas, USA.

**[43]** Champion, C., & Liel, A. (2012). The Effect of Near-fault Directivity on Building Seismic Collapse Risk. Earthquake Engineering & Structural Dynamics, 41(10), 1391-1409.

**[44]** American Society of Civil Engineers. (2017). ASCE/SEI 41-17: Seismic Evaluation and Retrofit of Existing Buildings Seismic Rehabilitation.

**[45]** Powell, G. H., & Allahabadi, R. (1988). Seismic Damage Prediction by Deterministic Methods: Concepts and Procedures. Earthquake Engineering & Structural Dynamics, 16(5), 719-734.

**[46]** Krawinkler, H., & Zohrei, M. (1983). Cumulative Damage in Steel Structures Subjected to Earthquake Ground Motions. Computers & Structures, 16, 531-541.

**[47]** Nabid, N., Hajirasouliha, I., & Petkovski, M. (2018). Performance-based Optimisation of RC Frames with Friction Wall Dampers Using a Low-cost Pptimisation Method. Bulletin of Earthquake Engineering, 16(10), 5017-5040.

**[48]** Moghaddam, H., Hajirasouliha, I., & Doostan, A. (2005). Optimum Seismic Design of Concentrically Braced Steel Frames: Concepts and Design Procedures. Journal of Constructional Steel Research, 61(2), 151-166.

**[49]** De Domenico, D., & Hajirasouliha., I. (2021). Multi-level Performance-based Design Optimisation of Steel Frames with Nonlinear Viscous Dampers. Bulletin of Earthquake Engineering, 19(12), 5015-5049.

**[50]** FEMA 356, F. E. (2000). Prestandard and Commentary for the Seismic Rehabilitation of Buildings. Federal Emergency Management Agency: Washington, DC, USA.

**[51]** Eads, L., Miranda, E., Krawinkler, H., & Lignos, D. G. (2013). An Efficient Method for Estimating the Collapse Risk of Structures in Seismic Regions. Earthquake Engineering & Structural Dynamics, 42(1), 25-41.

**[52]** Taslimi, A., & Tehranizadeh, M. (2022). The Effect of Vertical Near-field Ground Motions on the Collapse Risk of High-rise Reinforced Concrete Frame-core Wall Structures. Advances in Structural Engineering, 25(2), 410-425.